PIEZOELECTRIC PROPERTIES OF ScAlN THIN FILMS FOR PIEZO-MEMS DEVICES

Keiichi Umeda[1], H. Kawai[1], A. Honda[1], M. Akiyama[2], T. Kato[1] and T. Fukura[1]
[1]Murata Manufacturing Co., Ltd., Japan
[2]National Institute of Advanced Industrial Science and Technology, Japan

ABSTRACT

This paper reports the piezoelectric properties of ScAlN thin films. We evaluated the piezoelectric coefficients d_{33} and d_{31} of $Sc_xAl_{1-x}N$ thin films directly deposited onto silicon wafers, as well the radio frequency (RF) electrical characteristics of $Sc_{0.35}Al_{0.65}N$ bulk acoustic wave (BAW) resonators at around 2 GHz, and found a maximum value for d_{33} of 28 pC/N and a maximum $-d_{31}$ of 13 pm/V at 40% scandium concentration. In BAW resonators that use $Sc_{0.35}Al_{0.65}N$ as a piezoelectric film, the electromechanical coupling coefficient k^2 (=15.5%) was found to be 2.6 times that of resonators with AlN films. These experimental results are in very close agreement with first-principles calculations. The large electromechanical coupling coefficient and high sound velocity of these films should make them suitable for high frequency applications.

INTRODUCTION

M. Akiyama *et al.* developed $Sc_{0.43}Al_{0.57}N$ thin films with piezoelectric coefficients ~400% higher than those of AlN films [1]. Using quantum mechanical analysis, F. Tasnádi *et al.* discovered that this increase is caused by a strong change in the response of internal atomic coordinates to strain, and used this to calculate the piezoelectric coefficient e_{33} and the elastic stiffness c_{33} [2]. The radio frequency (RF) electrical characteristics of $Sc_{0.15}Al_{0.85}N$ BAW resonators [3], $Sc_{0.12}Al_{0.85}N$ BAW resonators [4], and $Sc_{0.46}Al_{0.54}N$ SAW resonators [5] have also been assessed. In this paper, the coefficients d_{33} and d_{31} of $Sc_xAl_{1-x}N$ thin films are calculated for values of x from 0 to 0.5, and the electromechanical coupling coefficient, relative dielectric constant, temperature coefficient of elastic stiffness, and velocity of sound in a $Sc_{0.35}Al_{0.65}N$ BAW resonator are given for the first time.

SPUTTERING PROCESSES

$Sc_xAl_{1-x}N$ thin films that were strongly oriented along the c-axis were prepared on (100) silicon substrates using two different sputtering methods: radio frequency magnetron reactive sputtering at a single target at 200 °C [6] and dual radio frequency magnetron reactive co-sputtering at 400 °C [1].

In the RF frequency magnetron reactive sputtering method, a 152.4 mm diameter aluminum sputtering target into which scandium chips have been partially embedded is used. In this process, the concentration of Sc in the thin films is adjusted by controlling the positioning and the density of Sc chips within the Al target. Prior to deposition, the sputtering chamber is evacuated to a pressure below 1.0×10^{-4} Pa, and then nitrogen at 40% concentration and argon are introduced. RF sputtering at 1500 W is then performed. Finally, the target is cleaned under deposition conditions for five minutes with the shutter closed. This method is mainly used to fabricate BAW resonators.

In the dual radio frequency magnetron reactive co-sputtering process, the Sc concentration is controlled by regulating the power level at the Al and Sc targets, each 50.8 mm in diameter, in a sputtering chamber that is evacuated to a pressure below 1.2×10^{-6} Pa. This method is used to investigate the dependence of the piezoelectric coefficients d_{33} and d_{31} on Sc concentration.

BAW FABRICATION PROCESS

Figure 1 shows a cross-sectional view of the BAW resonator. In the fabrication process, a 0.5-μm Cu layer is first deposited onto the substrate and patterned; this layer serves as a sacrificial layer in order to create an air gap. A 0.9 μm piezoelectric layer of $Sc_{0.35}Al_{0.65}N$ film or AlN film is then deposited and pattered. The piezoelectric film is sandwiched between 0.15-μm-thick Pt/Au/Pt top and bottom electrodes that can be used to excite the fundamental thickness longitudinal vibration modes in the resonator. A 0.1-μm-thick SiN film is added on both sides of the resonator using plasma enhanced chemical vapor deposition (PECVD) to serve as a protective layer.

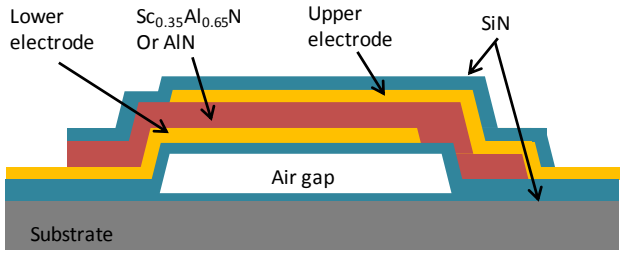

Figure 1.A schematic view of the BAW resonator

FIRST-PRINCIPLES CALCULATION

The piezoelectric properties of a $Sc_xAl_{1-x}N$ film were derived from first-principles calculations based on density functional perturbation theory [8] using a Vienna Ab-initio Simulation Package (VASP) [9]. A generalized gradient approximation of characteristics including spin polarization was used to calculate exchange-correlation energy [10] based on the atomic potentials of the projector augmented wave type [11] and a plane wave basis set at a cut-off energy of 500 eV. All of the calculations were performed using a $6 \times 6 \times 4$ k-point mesh that included the Γ-point of the first Brillouin zone. A $2 \times 2 \times 2$ supercell of AlN with a wurtzite structure, in which scandium atoms were substituted at aluminum sites in a manner such that the inter-scandium atomic distance was maximized, was then prepared. Figure 2 shows the crystalline composition

of the $Sc_xAl_{16-x}N_{16}$ structure used in this study (where x ranges from 0 to 16). For all structures used, the lattice vectors and the positioning of the atoms were optimized using first-principles calculations prior to calculating their piezoelectric properties.

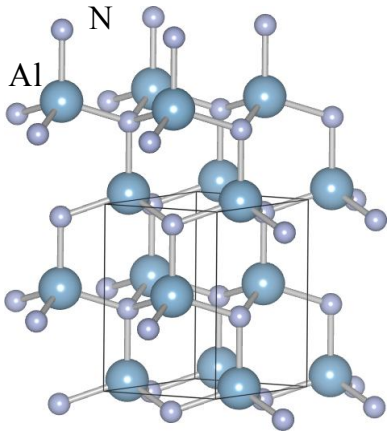

Figure 2. Wurtzite structure of $Sc_xAl_{16-x}N_{16}$ (x = 0)

EVALUATION

The scandium concentration in the films was analyzed using a wavelength dispersive X-ray fluorescence spectrometer (WDX).

The Si substrates composing the bottom electrodes, which were used for evaluating the piezoelectric coefficients d_{33} and d_{31}, had a resistivity of 0.01 ohm· cm. $Sc_xAl_{1-x}N$ thin films were directly deposited onto this Si substrate, and then a top electrode of Ti was deposited onto the $Sc_xAl_{1-x}N$ layer. The piezoelectric coefficient d_{33} of the $Sc_xAl_{1-x}N$ thin films were measured using a piezometer system (PM300 Piezotest) that sandwiched samples between two electrodes (Figure 3), while the coefficients d_{31} were obtained using a wafer flexure method [7] in which a driving *ac* field applied to the films in the z-direction caused stress in the xy-plane, changing the shape of the substrates (as shown in Figure 4). The displacement caused by substrate bending was measured with a laser Doppler vibrometer.

The RF electrical characteristics of the scattering parameter S_{11} were measured using a network analyzer and a probe station with a heater stage. Scattering data were obtained at 23, 50, and 85 °C in order to evaluate the temperature coefficients at anti-resonant frequency (TCF_f_p) and the c_{33} elastic stiffness (TCE_c_{33}) for $Sc_{0.35}Al_{0.65}N$ films. The piezoelectric properties extracted from the measurement data of BAW resonators were analyzed using a Mason's equivalent circuit (transmission line) model [12], which can be applied to one-dimensional, multi-layer resonators.

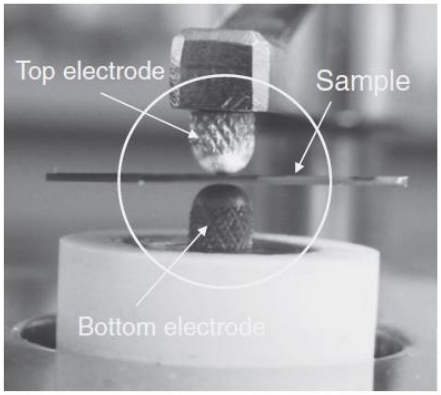

Figure 3. A photograph showing the setup for d_{33} measurement

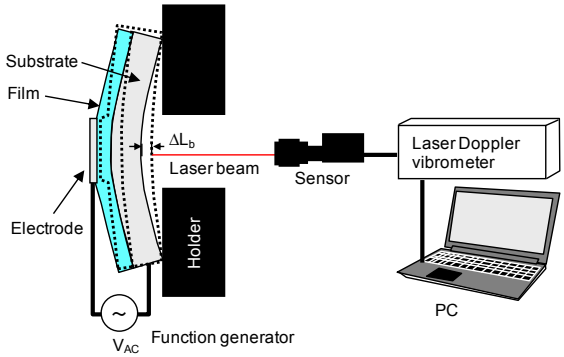

Figure 4. A schematic view of bending displacement measurement using a laser Doppler vibrometer

EXPERIMENTAL RESULTS

Figure 5 shows the values of the piezoelectric coefficient d_{33} in $Sc_xAl_{1-x}N$ thin films deposited by both single and dual target sputtering methods. The maximum recorded d_{33} of 28 pC/N is consistent with previous results [1], [13], and it was found that the values of d_{33} were the same for each of the sputtering methods.

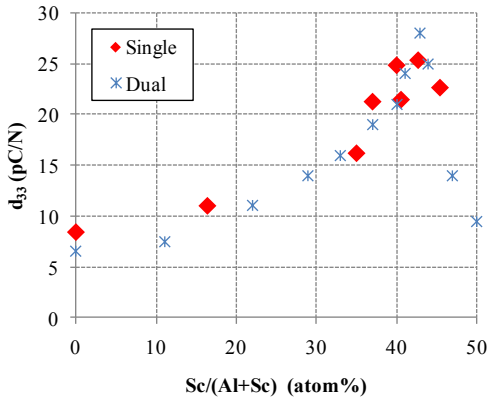

*Figure 5. Dependence of piezoelectric coefficient d_{33} on Sc concentration for $Sc_xAl_{1-x}N$ thin films. (red point ◆: single Al target embedded Sc chips, blue points *: Al and Sc dual target)*

Figures 6 and 7 show the dependence of the piezoelectric coefficients d_{33} and $-d_{31}$, respectively, on Sc concentrations as obtained by measurement and first-principles calculations.

As shown in Figure 7, a piezoelectric coefficient $-d_{31}$ of 13 pm/V is obtained at 40% scandium concentration. The coefficients d_{33} and $-d_{31}$ both increase in a nonlinear fashion with increasing scandium concentration.

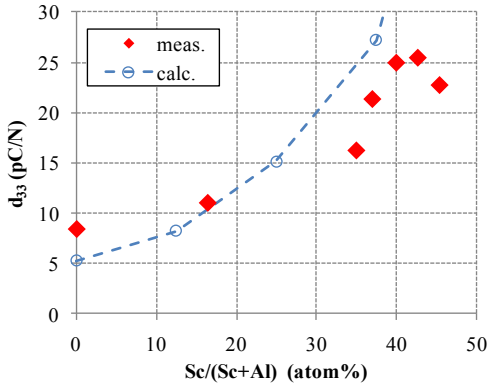

Figure 6. Dependence of piezoelectric coefficient d_{33} on Sc concentration for $Sc_xAl_{1-x}N$ thin films. Comparison between the measurement and first-principles calculation data.

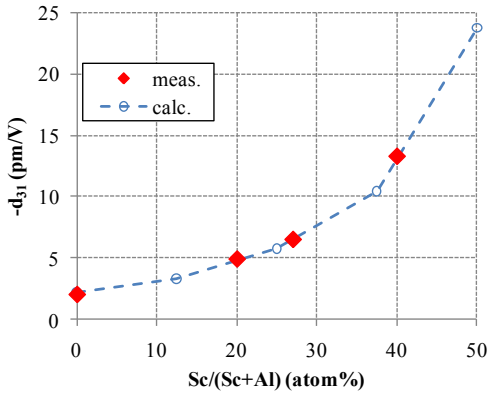

Figure 7. Dependence of piezoelectric coefficient d_{31} on Sc concentration for $Sc_xAl_{1-x}N$ thin films. Comparison between the measurements and the first principle calculations data.

Typical measured electrical characteristics of the $Sc_{0.35}Al_{0.65}N$ BAW resonator at resonance frequency (2 GHz) are shown in Figure 8, in which the red and blue lines show the impedance and phase, respectively.

The temperature characteristics of the resonator at the anti-resonant frequency are shown in Figure 9. The relative band width $2(f_p-f_s)/(f_p+f_s)(\%)$ and the electromechanical coupling coefficient $k^2=\pi^2/4(f_s/f_p)(f_p-f_s)/f_p$ $(\%)$ where f_s is the resonant frequency and f_p is the anti-resonant frequency, are shown in Table 1. It can be seen that the value of the electromechanical coupling coefficient of $Sc_{0.35}Al_{0.65}N$ film is 2.6 times that of the AlN film. The lower resonant frequency of the $Sc_{0.35}Al_{0.65}N$ BAW resonator as compared to that of the AlN BAW even at equal film thicknesses indicates that the elastic stiffness of the former is smaller, while the larger TCF_f_p value seen in the $Sc_{0.35}Al_{0.65}N$ BAW resonator is possibly caused by softening.

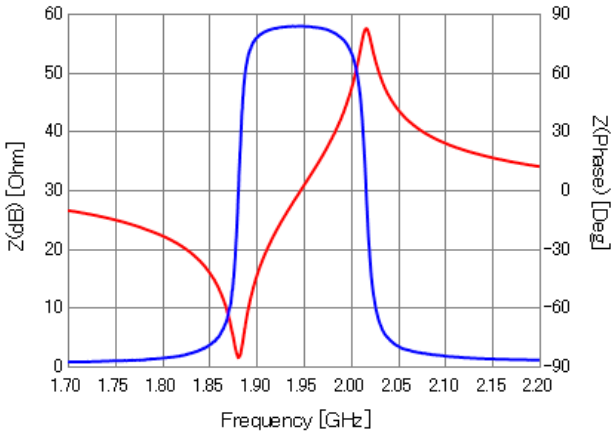

Figure 8. Measured electrical characteristics of the $Sc_{0.35}Al_{0.65}N$ BAW resonator (red line: impedance curve, blue line: phase curve)

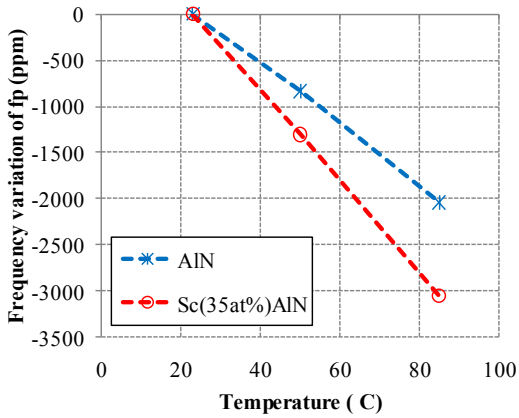

*Figure 9. Temperature characteristics of the anti-resonant frequency (red point ○: $Sc_{0.35}Al_{0.65}N$ BAW resonator, blue points *: AlN BAW resonator)*

Table 1: Measurement data of BAW resonators

	Measurement data of BAW resonator			
	Relative B.W.(%)	k^2(%)	Resonant frequency (MHz)	TCF_f_p (ppm/K)
AlN	2.4	5.8	2398	-32
$Sc_{0.35}Al_{0.65}N$	7.0	15.5	1880	-49

Table 2 shows piezoelectric film properties extracted from measurement data by fitting them to Mason's equivalent circuit model, with typical ZnO data shown for comparison. The longitudinal wave velocity (V_L) shown in Figure 10 is derived from $V_L=(c_{33}/\rho)^{1/2}$, where ρ is density. It can be seen that $Sc_{0.35}Al_{0.65}N$ films have larger piezoelectric coefficients d_{33} and TCE_c_{33} and lower longitudinal wave velocity than do AlN films, as well as larger d_{33} , higher V_L, and lower TCE_c_{33} than ZnO films.

Table 2: Film properties of AlN and $Sc_{0.35}Al_{0.65}N$ extracted from their electrical characteristics

	Piezoelectric film properties				
	ε_r	d_{33} (pC/N)	c_{33} (GPa)	TCE_c_{33} (ppm/K)	Longitudinal wave velocity (m/s)
AlN	10	7	395	-60	10,941
$Sc_{0.35}Al_{0.65}N$	15	16	244	-100	8,509
ZnO (ref.)	10	11	218	-123	6,080

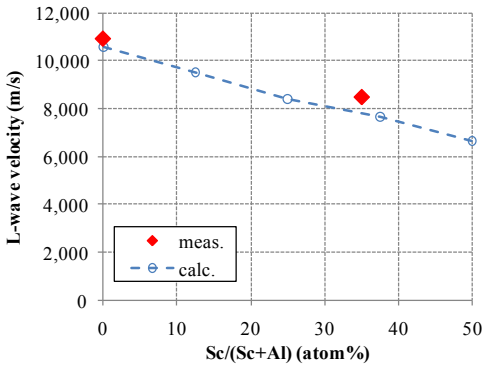

Figure. 10. Dependence of longitudinal wave velocity on Sc concentration for $Sc_xAl_{1-x}N$ thin films. Comparison between measurement and the first-principles calculation data.

The first-principles calculation data of d_{33}, d_{31}, and V_L as functions of scandium concentration for $Sc_xAl_{1-x}N$ thin films are plotted together with experimental data in Figures 6, 7, and 10, from which it can be seen that the calculated values are closely coincident with the experimental values. Figure 11 shows the calculated values of the *c/a* lattice constant ratio in $Sc_xAl_{1-x}N$, showing that increasing the Sc concentration decreases *c/a*. This effect might be caused by an expansion of the tetrahedral structure of AlN_4 along the a-axis, with a corresponding contraction along c-axis: As a result of this effect, Al atoms are more mobile along the c-axis, leading to an increase in the piezoelectric coefficients d_{33} and d_{31} and a decrease in elastic stiffness c_{33}.

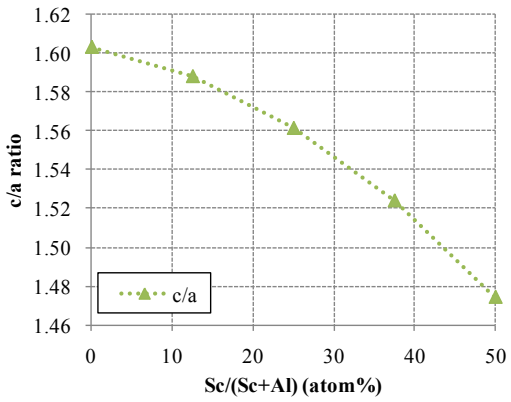

Figure.11. Dependence of c/a lattice constant ratio on Sc concentration for $Sc_xAl_{1-x}N$ thin films.

CONCLUSION

We have succeeded in revealing the properties of piezoelectric coefficients d_{33}, d_{31} and the longitudinal wave velocity V_L in $Sc_xAl_{1-x}N$ thin films by comparing observations with first principle calculations. Evaluating BAW resonators, we have shown for the first time that the k^2 value of a $Sc_{0.35}Al_{0.65}N$ film (15.5%) is 2.6 times that of an AlN film.

Owing to their large value of k^2 and high V_L, $Sc_xAl_{1-x}N$ films show potential for use in piezo-microelectromechanical systems (MEMS) devices, even when deposited by simple sputtering methods at low temperatures of around 200 °C. In particular, $Sc_xAl_{1-x}N$ films would be promising materials for use in high frequency and large bandwidth resonators and filters if it were possible to solve the problem of frequency drift against temperature caused by large *TCE_*c_{33}. SiO_2 has a temperature coefficient of Young's modulus (*TCE)* that is opposite to that of $Sc_xAl_{1-x}N$, and a proper composition of these two materials might be used to compensate for the temperature dependence at resonance frequency [14].

REFERENCES

[1] M. Akiyama, K. Kano and A. Teshigawara, Appl. Phys. Lett. 95, 162107 (2009).

[2] F. Tasnádi, B. Alling, Carina Höglund, G. Wingqvist, J. Birch, L. Hultman and I. A. Abrikosov, Phys. Rev. Lett. 104, 137601 (2010).

[3] M. Moreira, J. Byurström, I. Katardjev and V. Yantchev, Vacuum 86 (2011), pp. 23-26.

[4] R. Matloub, A. Artieda, C. Sandu, E. Milyutin and P. Muralt, Appl. Phys. Lett. 99, 092903 (2011).

[5] K. Hashimoto, S. Sato, A. Teshigawara, T. Nakamura and K. Kano, Proc. IEEE International Microwave Symposium (2012).

[6] K. Umeda, M. Takeuchi, H. Yamda, R. Kubo and Y. Yoshino, Vacuum 80, 658 (2006)

[7] A. L. Kholkin et al., Rev. Sci. Instrum. 67, 1935 (1996).

[8] S. Baroni, S. Gironcoli, and A. Corso, Rev. Mod. Phys. 73, 515 (2001).

[9] G. Kresse, and J. Furthmuller, Phys. Rev. B 59, 11169 (1996).

[10] J. P. Perdew, K. Burke, and M. Ernzerhof, Phys. Rev. Lett. 77, 3865 (1996).

[11] G. Kresse, and D. Joubert, Phys. Rev. B 59, 1758 (1999).

[12] W. P. Mason, Piezoelectric Crystals and Their Applications to Ultrasonics. D. Van Nostrand, 1950

[13] M. Akiyama, T. Kamohara, K. Kano, A. Teshigahara, Y. Takeuchi, and N. Kawahara, Adv. Mater. 21, 593 (2009).

[14] M. Kadota, T. Nakao, N. Taniguchi, E. Takata, M. Mimura, K. Nishiyama, T. Hada, and T. Komura: Proc. IEEE Ultrasonics Symp., p. 1970. (2004)

CONTACT

Keiichi Umeda
Murata Manufacturing Co., Ltd.
Tel: +81-77-586-8187; Fax: +81-77-587-6782
E-mail: k_umeda@murata.co.jp